Microtopographical effects of natural scaffolding on cardiomyocyte function and arrhythmogenesis

U. Shah[a,b], **H. Bien**[a,b], and **E. Entcheva**[a,c,*]

[a]Department of Biomedical Engineering, Stony Brook University, Stony Brook, NY 11794-8181, USA

[b]School of Medicine, Stony Brook University, Stony Brook, NY 11794-8181, USA

[c]Department of Physiology and Biophysics, Stony Brook University, Stony Brook, NY 11794-8181, USA

Abstract

A natural myocardial patch for heart regeneration derived from porcine urinary bladder matrix (UBM) was previously reported to outperform synthetic materials (Dacron and expanded polytetrafluoroethylene (ePTFE)) used in current surgical treatments. UBM, an extracellular matrix prepared from urinary bladder, has intricate three-dimensional architecture with two distinct sides: the luminal side with a smoother surface relief; and the abluminal side with a fine mesh of nano- and microfibers. This study tested the ability of this natural scaffold to support functional cardiomyocyte networks, and probed how the local microtopography and composition of the two sides affects cell function. Cardiomyocytes isolated from neonatal rats were seeded *in vitro* to form cardiac tissue onto luminal (L) or abluminal (Ab) UBM. Immunocytochemistry of contractile cardiac proteins demonstrated growth of cardiomyocyte networks with mature morphology on either side of UBM, but greater cell compactness was seen in L. Fluorescence-based imaging techniques were used to measure dynamic changes in intracellular calcium concentration upon electrical stimulation of L and Ab-grown cells. Functional differences in cardiac tissue grown on the two sides manifested themselves in faster calcium recovery ($p < 0.04$) and greater hysteresis (difference in response to increasing and decreasing pacing rates) for L vs Ab side ($p < 0.03$). These results suggest that surface differences may be leveraged to engineer the desired cardiomyocyte responses and highlight the potential of natural scaffolds for fostering heart repair.

Keywords

Urinary bladder matrix; Scaffolding; Cardiomyocytes; Topography; Electrical stability

*Corresponding author. Address: Department of Biomedical Engineering, Stony Brook University, Stony Brook, NY 11794-8181, USA. Tel.: +1 631 444 2368; fax: +1 631 444 6646. emilia.entcheva@sunysb.edu (E. Entcheva).

1. Introduction

Cardiac tissue is terminally differentiated and therefore has limited repair and regeneration ability in the event of disease or injury. Cardiovascular disease, more specifically ischemic heart disease, remains a leading cause of death for adults throughout the world [1]. Definitive care usually requires whole heart transplantation, but the insufficiency of donor organs necessitates another approach. One alternative is a surgical technique, the Dor procedure, in which infarcted myocardium is replaced with an inert patch [2]. Typically, the patch is composed of biologically inert woven polyethylene terephthalate fibers (Dacron) [3]. Dacron is well tolerated by the body, has high tensile strength and high resistance to stretching and degradation in wet and dry forms [4]. However, Dacron's limitations include mineralization, fibrosis, risk of infection and its inability to become a functional constituent of the heart portion it replaces [5]. These drawbacks are shared by other synthetic scaffolds, precluding full integration within the cardiac muscle. Therefore, an alternative material that is biocompatible, biodegradable and can be replaced by host-derived tissue to restore cardiac function is in demand.

A potential candidate is natural scaffolding derived from an extracellular matrix (ECM). ECM serve as natural scaffolds for all organ and tissue growth; they are composed of various structural and functional proteins, growth factors, glycosaminoglycans and cytokines [6] arranged in a three-dimensional architecture which facilitates cell maturation. The composition and topography of ECM are essential in determining specificity, cellular structure, organization and function. Finally, ECMs' natural self-degradation allows regenerated tissue to exist on its own after maturation [5].

Naturally derived scaffolding with little to no immunological response can be prepared by careful removal of overlying tissue and cells to preserve ECM structure and composition. Various tissue types have been repaired with such natural scaffolding, including the lower urinary track, the esophagus, dura matter, blood vessels and musculotendinous tissues [5]. In fact, ECM scaffolding has been previously reported to outperform Dacron and ePTFE as a ventricular patch, and to aid in the improvement of overall heart function [7–9].

There are currently two commercially available acellular ECM scaffold materials: one is derived from porcine urinary bladder (UBM) (A-Cell, Jessup, MD), and the other porcine jejunum small intestinal submucosa (SIS) (Cook Biotech, West Lafayette, IN). SIS is rich in epithelial cells, tends to be well vascularized and is composed primarily of type I collagen [5]. UBM is extracted from the region below the smooth muscle cells along the lining of the bladder, and is composed mostly of type IV collagen, laminin and entactin [10]. Of the structural proteins, cardiomyocytes adhere most readily to collagen IV and laminin [11]. Furthermore, the growth factors within UBM include VEGF [12] and PDGF [13], which are critical for induction of angiogenesis, especially essential for highly oxygen-demanding heart tissue.

Another characteristic of UBM which may support heart tissue growth is its structure, composed of two different sides: one with a mesh of random fibers (abluminal side) and the other a flat base (luminal side). This is in contrast to Dacron's regular woven surface (Fig.

1). UBM's "loose" and fine fiber configuration with high porosity results in a high surface-to-volume ratio and thus potentially larger surface area for cell growth. These characteristics are suspected to play a significant role in enhancing cell adhesion and packing [14], thus promoting high cell density – essential for electrical and mechanical synchronization within cardiac tissue.

Based on these qualifications, it was hypothesized that UBM may serve as a suitable scaffolding material for engineering cardiac tissue. The authors set out to determine whether UBM could provide the environment needed for electrical stability, and whether functional response of the cardiomyocytes is sensitive to the architecture of the two UBM sides.

2. Methods

2.1. Material preparation and cell culture

Acellular UBM was purchased from A-Cell (A-Cell Jessup, MD). UBM scaffolds were cut under sterile conditions to 6×12 mm scaffolds and were plated with neonatal cardiac myocytes on either the luminal (L) or abluminal (Ab) side. Primary myocyte culture was done as previously described [15–17]. Briefly, cells were isolated from 2–3-day-old rat pups by trypsin (US Biochemicals, Cleveland, OH) and collagenase (Worthington Biomedical, Lakewood, NJ) enzyme digestion. After centrifugation, the cells were resuspended in culture medium M199 (GIBCO, Carlsbad, CA) supplemented with L-glutamine (GIBCO), glucose (Sigma, St. Louis, MO), penicillin–streptomycin (Mediatech Cellgro, Kansas City, MO), vitamin B12 (Sigma), HEPES (GIBCO) and 10% fetal bovine serum (GIBCO). A 90-min preplating removed fibroblasts from the cell population. Finally, the cardiac myocytes were plated at a density of 400 k cm^{-2} onto the prepared UBM scaffolds. The cells remained in culture medium with 10% serum for days 1 and 2; after that, 2% serum was used instead to help select for myocyte maturation over endothelial cells and fibroblast growth. The medium was changed every other day [17,18]. Functional and structural tests were performed on days 4–6 after plating.

2.2. Structural characterization of cardiomyocytes

For immunocytochemistry, cells were fixed and permeabilized with 3.7% formaldehyde and 0.02% Triton-X 100 before being stained with a monoclonal mouse antibody against alpha-actinin (Sigma). Samples were visualized using goat anti-mouse antibody conjugated with fluorophore Alexa 488 (Molecular Probes) and imaged on a Zeiss Apotome deconvolution system.

2.3. Functional characterization of cardiomyocytes

As a marker for cellular contractility, changes in intracellular Ca^{2+} upon electrical stimulation were measured with a calcium-sensitive fluorescent dye. Cardiomyocytes were labeled with Fluo-4 AM (Invitrogen, Carlsbad, CA) at 8 μM for 20 min and washed for an additional 20 min. Samples were placed into a temperature-controlled chamber (30.5 ± 0.3 °C) and perfused with Tyrode's solution (1.3 mM $CaCl_2$, 5 mM glucose, 5 mM HEPES, 1 mM $MgCl_2$, 5.4 mM KCl, 135 mM NaCl, 0.33 mM NaH_2PO_4, pH 7.4) throughout the experiment [15–17].

Fluorescence signals were acquired with the Ionoptix myocyte system (Ionoptix, Milton, MA). Samples were electrically stimulated (10–15 V cm^{-1}, 5 ms biphasic pulses) via platinum electrodes embedded in the sides of the experimental chamber. To test cells' restitution properties (response to changing frequencies of stimulation), a dynamic restitution protocol was followed where cells were paced until steady-state (60 beats) at each frequency, while gradually increasing the rate from 0.5 Hz until loss of 1:1 capture. At each frequency, 20 transients were recorded during steady-state pacing. After loss of 1:1 response, pacing at decreasing frequencies back to 0.5 Hz was executed to test for hysteresis (difference in the response depending on pacing history: upward or downward change in frequency).

2.4. Computational analysis: calcium transient morphology

Analysis software was used to filter the acquired signals and to extract several parameters characterizing Ca^{2+} transient morphology: maximum departure velocity (dep v), departure velocity time (dep v t), peak height (peak h), time to reach peak height (peak t), maximum return velocity (ret v), time of maximum return velocity (ret v t), and time to repolarize to 50% (t to bl 50%) and 80% (t to bl 80%), i.e., calcium transient duration (CTD), CTD50 and CTD80, respectively (Fig. 2). Student's *t*-test was used to determine the statistical significance between the cell response on both sides of the UBM; $p < 0.05$ was considered significant.

2.5. Hysteresis quantification

Recently, there has been interest in quantifying the memory or hysteresis in the dynamic response of cardiac tissue [19]. This is achieved by comparing restitution properties (CTD vs diastolic interval (DI)) [20] upon acceleration of pacing rate (up) and upon deceleration of rate (down). A difference between the two curves is indicative of the presence of hysteresis, and may also be used to predict resistance to arrhythmias [21,22].

Calcium hysteresis was quantified by first constructing CTD vs DI restitution curves through a non-linear curve-fitting procedure (Matlab):

$$\text{CTD} = \text{CTD}_{\text{Max}} - m * e^{-\frac{(\text{DI} - \text{DI}_{\text{min}})}{\tau}} \quad (1)$$

where DI represents diastolic interval, CTD calcium transient duration, τ a time constant, and *m* the slope. Thereafter, the area between the up and down restitution curves after the initial intersection point was measured via analytical integration in Maple (Maplesoft, Waterloo, Canada).

3. Results and discussion

The first aim of this study was to assess whether cardiomyocytes could successfully grow on UBM to form connected networks and simulate tissue formation *in vitro*. The second aim was to determine whether the distinct local microtopography of the two sides of UBM scaffolding affects the growth and function of the cardiomyocytes. This information could be used to guide future scaffold design and ultimately for proper surgical implantation of the matrix for heart repair, particularly in cases with cell seeding.

Imaging of sarcomeric actinin revealed that myocytes grew well on both sides of the material (Fig. 3), forming mature tissue, as evidenced by the striations and well-developed sarcomeres, especially on the luminal side of the UBM scaffold (Fig. 3D). Furthermore, no additional protein coating was necessary to promote cell adhesion, as is often essential with many synthetic scaffold materials [23]. Overall, cells tended to grow following the surface structure. This resulted in myocytes on the abluminal side (Fig. 3A and C) with a mesh-like architecture having a sparser appearance with more complex connectivity and atypical cell extensions compared with the luminal side (Fig. 3B and D), which offered higher in-plane compactness.

To assess the functionality of the tissue constructs, intracellular calcium measurements from 14 abluminal and 14 luminal samples were assessed. Differences in transient morphology between the two sides are shown in Fig. 4A. Calcium transients of cardiomyocytes plated on the luminal side exhibited a trend for shorter transient duration, larger peak height and faster departure and return velocities, the differences in the return velocity were significant ($p < 0.04$) (Fig. 4B and C). Faster return velocity is associated with timely removal of calcium from the cytoplasm to prepare for the next contraction. Removal of calcium from the cytoplasm is controlled by two major processes: the SERCa pump refills the sarcoplasmic reticulum Ca^{2+} stores, and the Na^+/Ca^{2+} exchanger extrudes Ca^{2+} outside the cell. Impairment or rudimentary function of either of these two proteins (often found in heart failure, for example) may lead to slower Ca^{2+} transient recovery, closer to that seen in the Ab-cells (Fig. 4). Alternatively, the reduced compactness due to the complex surface in Ab-cells most likely led to reduced connectivity, thus prolonging transient duration and decreasing departure and return velocities.

When engineering cardiac tissue, one has to ensure functional safety. It is especially critical for an implantable cardiac patch to be resistant to arrhythmia generation [24–27]. Wu and Patwardhan [21] demonstrated that the presence of hysteresis in the relationship action potential duration (APD) vs DI might reduce electrical instabilities (alternans) and thus help prevent malignant arrhythmias such as ventricular fibrillation [22]. Hysteresis is short-term cardiac memory or dependence of the current electrical pulse from previous beats, and was chosen as an indirect measure of electrical stability. The duration of the intracellular calcium transients (CTD) was used instead of APD with the assumption that under control conditions the synchrony between APD and calcium duration does not break [28]. The present analysis indicated the presence of hysteresis in cardiac tissue developed on both UBM sides; however, the L side exhibited significantly higher hysteresis (Fig. 5). These findings confirm the functional competency of cardiac syncytium grown on UBM scaffolding, particularly on the luminal side.

This study corroborates the potential advantages of natural scaffolding for cardiac tissue repair that have been highlighted previously [7–9]. Cell microenvironment affects cell function and is critical for inducing cell proliferation and differentiation. For example, human mesenchymal stem cells cultured on a basement ECM exhibit an increased proliferation rate compared with growth on plastic [29]. Acellular natural scaffolding was also shown to attract bone marrow derived cells [30] and endothelial progenitor cells circulating in the peripheral blood [31,32]. The latter is essential in promoting local

vascularization for the metabolically active myocardium. UBM's ability to attract possible progenitor cells has been demonstrated in previous studies. Furthermore, Kochupura et al. [9] found that the use of UBM as a right ventricular patch promoted the development of cardiomyocyte population in the region of the patch, unlike the synthetic Dacron. Similarly, UBM outperformed ePTFE by fostering cardiac tissue repair with less fibrosis, calcification and foreign-body giant cell reactions; formation of mature cardiomyocytes resulted in the UBM region, but not with the ePTFE [7]. The use of UBM also led to superior functional performance (mechanical function) compared with synthetic scaffolding [7,9].

Cell pre-seeding of the scaffolding intended for cardiac repair can provide further improvement of function. For the UBM material tested in this study, the data indicate that the luminal side may be more suitable for cell seeding. The functional differences between cells grown on both sides may be due to the distinctly different surface topography (Fig. 1). A tendency for hypertrophy development as a complex function of scaffold topography was demonstrated previously [18,33]. The need for denser cell packing could lead to cardiomyocyte preference for the less fibrous luminal side; albeit fine fiber orientation (as opposed to random distribution) can facilitate better cardiac tissue growth [34]. In addition, the ECM protein composition of the two sides may influence cell adhesion, as discussed earlier [10]. A recent study of several natural matrices found that only the luminal UBM side offered intact basement membrane, essential for healing and cellular modeling, characterized by localized collagen VII within collagen IV and laminin [8], which is another factor to consider in cell seeding prior to patch implantation.

4. Conclusions

Overall, the data indicate compatibility of the UBM matrix with cardiomyocytes and support its potential for cardiac applications. While both sides supported the growth of well-connected cells with mature sarcomeric organization, an important finding here is that cardiomyocytes grow and function differently on the two sides of the UBM matrix, with the luminal side promoting more desirable functional properties. These results suggest that surface differences may be leveraged to engineer desired cardiomyocyte responses and highlight the potential of natural scaffolds for heart repair. Finally, an immediate use of UBM cardiac tissue patch can be sought as an *in vitro* test bed for pharmaceutical drugs, where they can be administered directly with minimum animal sacrifice and ethical compunction.

Acknowledgments

References

1. American Heart Association. Heart disease and stroke statistics – 2009 update. Dallas: AHA; 2009.

2. Athanasuleas CL, Buckberg GD, Stanley AW, Siler W, Dor V, Di Donato M, et al. Surgical ventricular restoration in the treatment of congestive heart failure due to post-infarction ventricular dilation. J Am Coll Cardiol. 2004; 44(7):1439–45. [PubMed: 15464325]

3. Iha K, Ikemura R, Higa N, Akasaki M, Kuniyoshi Y, Koja K. Left ventricular pseudoaneurysm after sutureless repair of subacute left ventricular free wall rupture: a case report. Ann Thorac Cardiovasc Surg. 2001; 7(5):311–4. [PubMed: 11743861]

4. Badylak S, Liang A, Record R, Tullius R, Hodde J. Endothelial cell adherence to small intestinal submucosa: an acellular bioscaffold. Biomaterials. 1999; 20(23–24):2257–63. [PubMed: 10614932]

5. Badylak S, Obermiller J, Geddes L, Matheny R. Extracellular matrix for myocardial repair. Heart Surg Forum. 2003; 6(2):E20–6. [PubMed: 12716647]

6. Hodde J, Record R, Tullius R, Badylak S. Fibronectin peptides mediate HMEC adhesion to porcine-derived extracellular matrix. Biomaterials. 2002; 23(8):1841–8. [PubMed: 11950054]

7. Robinson KA, Li J, Mathison M, Redkar A, Cui J, Chronos NA, et al. Extracellular matrix scaffold for cardiac repair. Circulation. 2005; 112(9 Suppl):I135–43. [PubMed: 16159805]

8. Brown B, Lindberg K, Reing J, Stolz DB, Badylak SF. The basement membrane component of biologic scaffolds derived from extracellular matrix. Tissue Eng. 2006; 12(3):519–26. [PubMed: 16579685]

9. Kochupura PV, Azeloglu EU, Kelly DJ, Doronin SV, Badylak SF, Krukenkamp IB, et al. Tissue-engineered myocardial patch derived from extracellular matrix provides regional mechanical function. Circulation. 2005; 112(9 Suppl):I144–9. [PubMed: 16159807]

10. Badylak SF. The extracellular matrix as a scaffold for tissue reconstruction. Semin Cell Dev Biol. 2002; 13(5):377–83. [PubMed: 12324220]

11. Borg, TK.; Terracio, L. Interaction of the extracellular matrix with cardiac myocytes during development and disease. In: Robinson, TF.; Kinne, RKH., editors. Cardiac myocyte-connective tissue interactions in health and disease. Basel, Switzerland: Karger; 1990. p. 113-30.

12. Richardson TP, Peters MC, Ennett AB, Mooney DJ. Polymeric system for dual growth factor delivery. Nat Biotechnol. 2001; 19(11):1029–34. [PubMed: 11689847]

13. Carmeliet P, Conway EM. Growing better blood vessels. Nat Biotechnol. 2001; 19(11):1019–20. [PubMed: 11689842]

14. Dahms SE, Piechota HJ, Dahiya R, Lue TF, Tanagho EA. Composition and biomechanical properties of the bladder acellular matrix graft: comparative analysis in rat, pig and human. Br J Urol. 1998; 82(3):411–9. [PubMed: 9772881]

15. Entcheva E, Bien H. Tension development and nuclear eccentricity in topographically controlled cardiac syncytium. Biomed Microdevices. 2003; 5(2):163–8.

16. Entcheva E, Bien H, Yin L, Chung CY, Farrell M, Kostov Y. Functional cardiac cell constructs on cellulose-based scaffolding. Biomaterials. 2004; 25(26):5753–62. [PubMed: 15147821]

17. Bien H, Yin L, Entcheva E. Cardiac cell networks on elastic microgrooved scaffolds. IEEE Eng Med Biol Mag. 2003; 22(5):108–12. [PubMed: 14699943]

18. Yin L, Bien H, Entcheva E. Scaffold topography alters intracellular calcium dynamics in cultured cardiomyocyte networks. Am J Physiol Heart Circ Physiol. 2004; 287(3):H1276–85. [PubMed: 15105172]

19. Walker ML, Wan X, Kirsch GE, Rosenbaum DS. Hysteresis effect implicates calcium cycling as a mechanism of repolarization alternans. Circulation. 2003; 108(21):2704–9. [PubMed: 14581412]

20. Weiss JN, Chen PS, Qu Z, Karagueuzian HS, Lin SF, Garfinkel A. Electrical restitution and cardiac fibrillation. J Cardiovasc Electrophysiol. 2002; 13(3):292–5. [PubMed: 11942602]

21. Wu R, Patwardhan A. Restitution of action potential duration during sequential changes in diastolic intervals shows multimodal behavior. Circ Res. 2004; 94(5):634–41. [PubMed: 14752029]

22. Berger RD. Electrical restitution hysteresis: good memory or delayed response? Circ Res. 2004; 94(5):567–9. [PubMed: 15031267]

23. Muschler GF, Nakamoto C, Griffith LG. Engineering principles of clinical cell-based tissue engineering. J Bone Joint Surg Am. 2004; 86-A(7):1541–58. [PubMed: 15252108]

24. Cristal N, Peterburg I, Szwarcberg J. Atrial fibrillation developing in the acute phase of myocardial infarction. Prognostic implications Chest. 1976; 70(1):8–11.

25. El Sherif N, Scherlag BJ, Lazzara R, Hope RR. Re-entrant ventricular arrhythmias in the late myocardial infarction period. 4. Mechanism of action of lidocaine. Circulation. 1977; 56(3):395–402. [PubMed: 69503]

26. Assayag P, Carre F, Chevalier B, Delcayre C, Mansier P, Swynghedauw B. Compensated cardiac hypertrophy: arrhythmogenicity and the new myocardial phenotype. I. Fibrosis Cardiovasc Res. 1997; 34(3):439–44.

27. Flinders DC, Roberts SD. Ventricular arrhythmias. Prim Care. 2000; 27(3):709–24. [PubMed: 10918676]

28. Bers, DM. Excitation–contraction coupling and cardiac contractile force. Dordrecht: Kluwer Academic Publishers; 1991.

29. Matsubara T, Tsutsumi S, Pan H, Hiraoka H, Oda R, Nishimura M, et al. A new technique to expand human mesenchymal stem cells using basement membrane extracellular matrix. Biochem Biophys Res Commun. 2004; 313(3):503–8. [PubMed: 14697217]

30. Badylak SF, Park K, Peppas N, McCabe G, Yoder M. Marrow-derived cells populate scaffolds composed of xenogeneic extracellular matrix. Exp Hematol. 2001; 29(11):1310–8. [PubMed: 11698127]

31. Ishikawa M, Asahara T. Endothelial progenitor cell culture for vascular regeneration. Stem Cells Dev. 2004; 13(4):344–9. [PubMed: 15345127]

32. Freedman SB, Isner JM. Therapeutic angiogenesis for coronary artery disease. Ann Intern Med. 2002; 136(1):54–71. [PubMed: 11777364]

33. Chung CY, Bien H, Entcheva E. The role of cardiac tissue alignment in modulating electrical function. J Cardiovasc Electrophysiol. 2007; 18(12):1323–9. [PubMed: 17916158]

34. Zong X, Bien H, Chung CY, Yin L, Fang D, Hsiao BS, et al. Electrospun fine-textured scaffolds for heart tissue constructs. Biomaterials. 2005; 26(26):5330–8. [PubMed: 15814131]

Appendix A. Figures with essential colour discrimination

Certain figures in this article, particularly Figures 2 and 3, are difficult to interpret in black and white. The full colour images can be found in the on-line version, at doi:10.1016/j.actbio.2010.02.041.
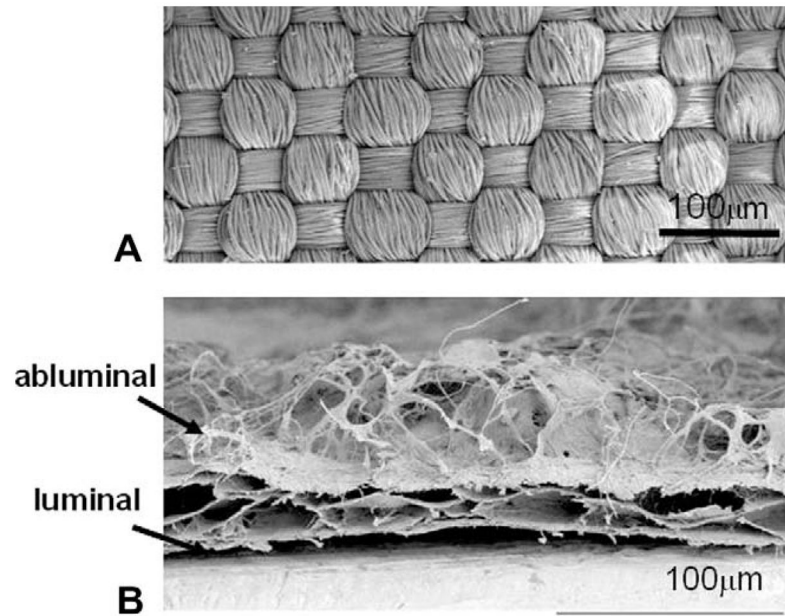
Fig. 1.
(A) SEM topical view of Dacron. (B) SEM cross-sectional view of UBM where layering of sheets is seen. Whereas the bottom (luminal side) is dense and flat, the top (abluminal) surface consists of a mesh of fibers without particular orientation. The density, length and thickness of the fibrous layer are non-uniform.
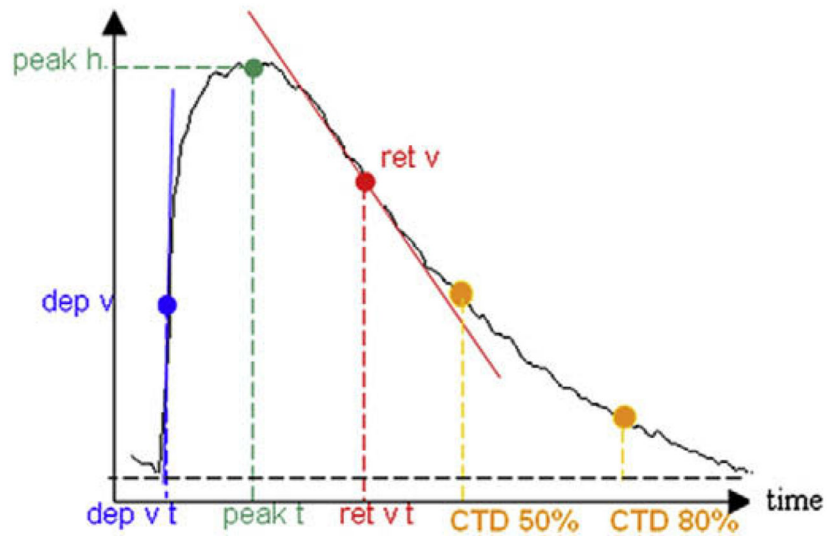
Fig. 2.
Example calcium transient with indication of quantified morphological characteristics, including temporal parameters (dep v t, ret v t, peak t, CTD50 and CTD80), as well as shape parameters (dep v, peak h and ret v). The transient parameter analysis was done using automated custom developed Matlab software. For further explanation, see the text.
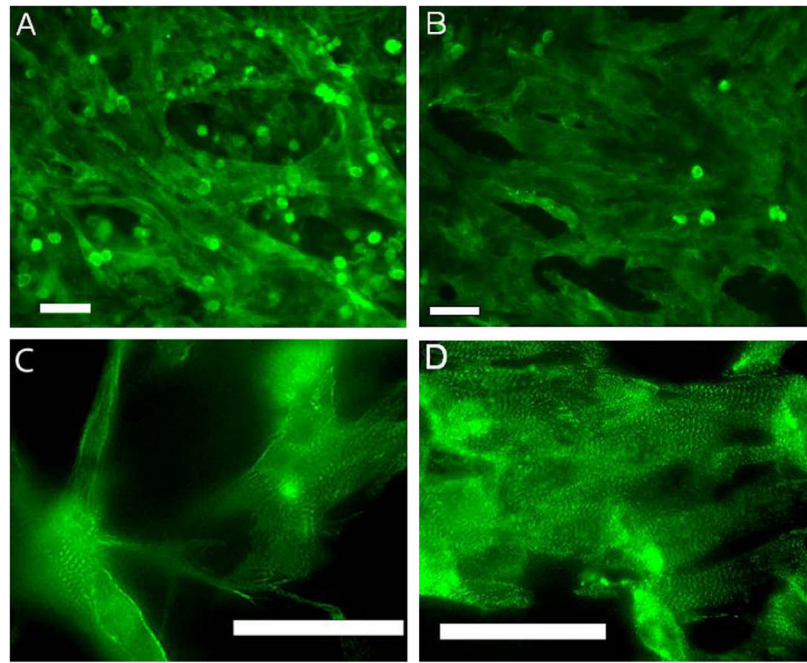
Fig. 3.
Cardiomyocytes seeded on the scaffolding and labeled with alpha-actinin: (A and C) cells seeded on the abluminal side of the scaffold; (B and D) cells seeded on the luminal side. While both sides supported the growth of connected cardiac tissue, overall higher cell density was observed on the luminal side (B). Higher magnification deconvolution images (C and D) reveal well-organized sarcomeres. In the abluminal case (C), some cell extensions/projections atypical for cardiomyocytes are seen due to the complex fibrous surface. All scale bars are 50 μm.
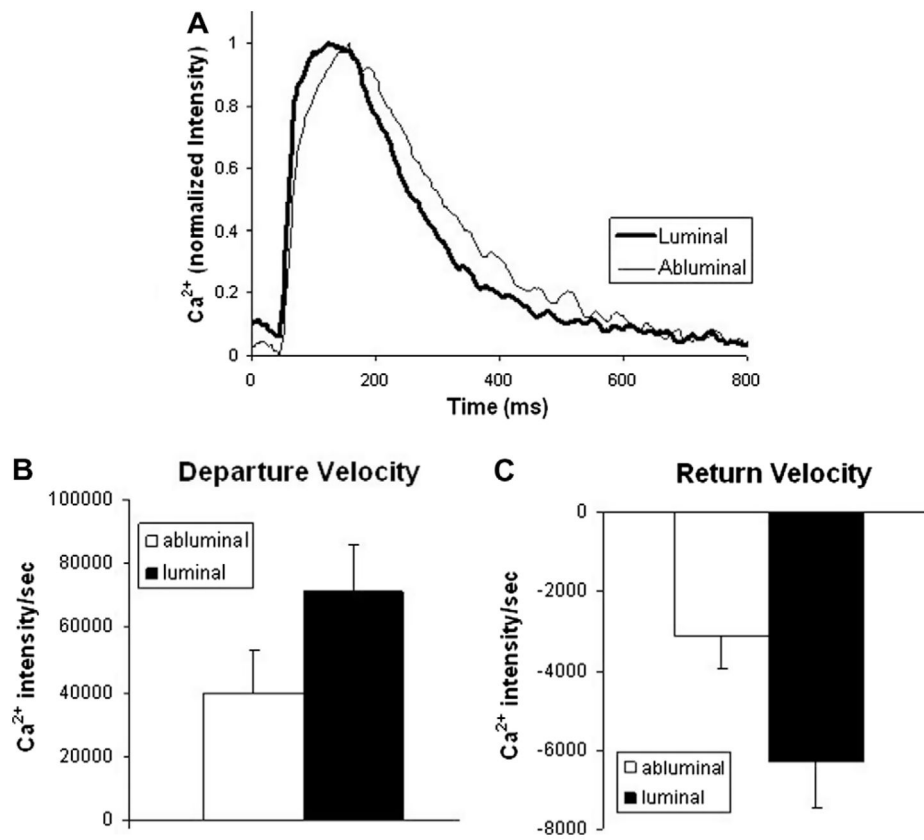
Fig. 4.
(A) Representative calcium transients (at 1 Hz pacing) from both sides of the UBM scaffolding. Transients from the luminal side show trends for shorter transient duration, larger peak height, and faster departure (B) and return velocities (C), indicating potentially superior calcium handling. Error bars show mean ± SE.
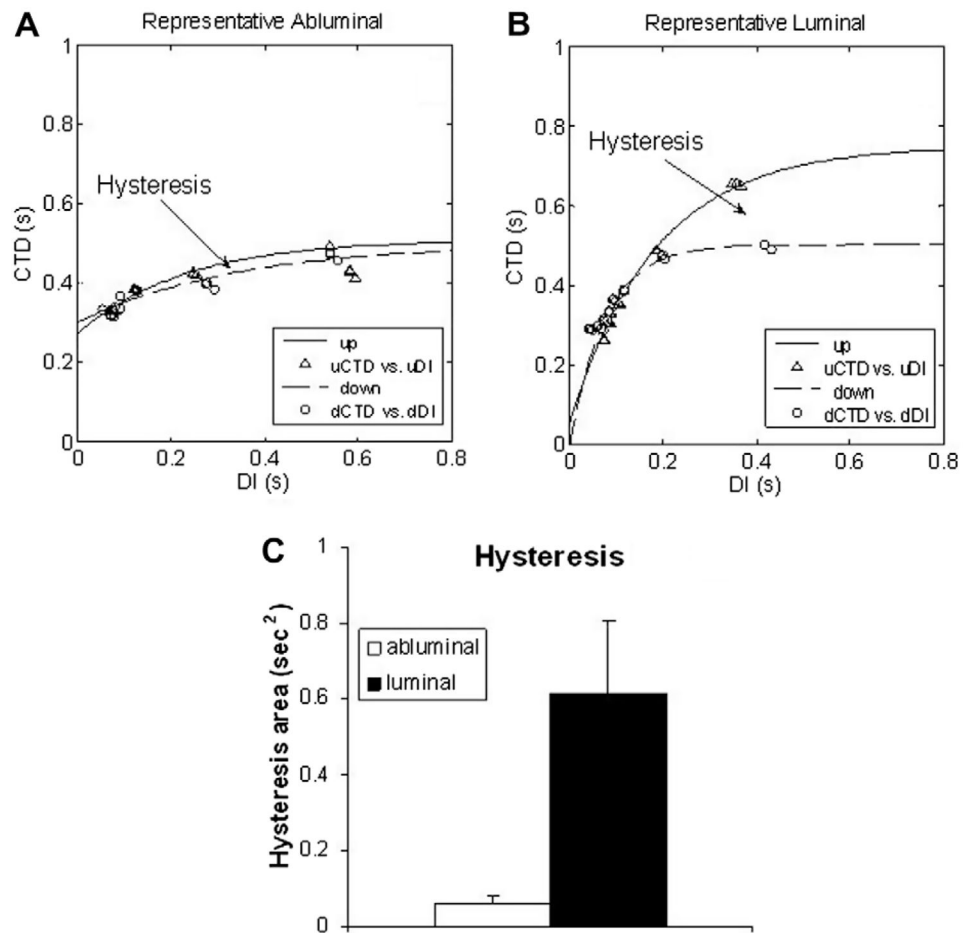
Fig. 5.
(A and B) Representative plots of the frequency response (CTD vs diastolic interval, DI) for myocardial cells plated on the abluminal and luminal side of the UBM, respectively. A hysteresis region is indicated in both cases, revealing difference in the response when pacing rate is progressively increasing vs decreasing. (C) A significantly larger amount of hysteresis was seen in cells seeded on the luminal side compared with the abluminal side ($p < 0.03$), which indicates potentially better electrical stability. Error bars show mean ± SE.